Journal of Applied Mechanics and Technical Physics, Vol. 46, No. 2, pp. 250–256, 2005

AEROSOL ASPIRATION INTO A CYLINDRICAL SAMPLER FROM A LOW-VELOCITY DOWNWARD FLOW AND FROM CALM AIR

M. V. Vanyunina, R. S. Galeev, Sh. Kh. Zaripov, and É. V. Skvortsov

UDC 532.529.6

The problem of aerosol aspiration into a two-dimensional cylindrical sampler from a low-velocity downward flow and from calm air is solved. A simple analytical model for the velocity field of the carrier medium in the vicinity of the sampler with allowance for the finite size of the input orifice is proposed. Parametric studies of the aspiration factor as a function of the Stokes number for different ratios of the free-stream and aspiration velocities and different gravity-induced sedimentation velocities for two positions of the sampler are performed. Sedimentation of particles on the lower side of the cylinder for the sampler with a downward-oriented orifice is discussed.

Key words: *aspiration, potential flow, cylindrical sampler.*

Introduction. Samplers with a blunt head, in particular, cylindrical samples, are often used to measure the concentrations of aerosol particles indoors. The interest is caused by the fact that the behavior of dust particles around a human head is similar to the behavior of particles during aspiration. Distortions of particle concentrations in aerosol measurements for different types of samplers and sampling conditions can predicted with the help of the aspiration factor. In the general case, the latter depends on the ratio of the free-stream velocity to the aspiration velocity, particle size and density, and geometric size and shape of the sampler. The results of theoretical and experimental investigations of the aspiration factor can be found in the monographs [1–3].

Under typical conditions of rather dusty atmospheric or room air, the fraction of aerosol particles is normally less than 10^{-6} of the air mass. Hence, the effect of aerosol particles on the gas flow can be neglected, and modeling of the aerosol flow with aspiration can be reduced to solving two problems: determination of the carrier-medium velocity field and calculation of particle trajectories in the resultant velocity field. Mathematical models for aspiration into cylindrical samplers were previously developed in [3–8]. The behavior of the trajectories of inertia-free aerosol particles in the vicinity of a cylindrical sampler in the case of aspiration from calm air was analyzed in [4, 8]. An analytical model (point sink on the cylinder) and a numerical model (aspiration through a finite-size slot) for calculating the aspiration factor within the framework of a potential flow of an incompressible fluid were proposed in [3, 5]. The models in the approximation of a viscous incompressible fluid flow were used to study the aspiration factor for a cylindrical sampler from a moving gas and from calm air in [6, 7]. The gas flow around cylindrical and spherical samplers and the aspiration factor were examined experimentally in [9, 10].

In the case of indoor measurements, the sampling was performed from a low-velocity gas flow or from calm air. Under these condition, an important factor that affects the aspiration process in addition to particle inertia is the force of gravity. Its influence on efficiency of aspiration into a spherical sampler was considered in [11, 12].

In the present work, we study the problem of aspiration into a cylindrical sampler from a low-velocity downward flow and from calm air. An analytical solution for the velocity field of the carrier medium in the vicinity of the sampler with allowance for the finite size of the input orifice is obtained within the framework of a potential

Chebotarev Institute of Mathematics and Mechanics, Kazan' State University, Kazan' 420008; shamil.zaripov@ksu.ru. Translated from Prikladnaya Mekhanika i Tekhnicheskaya Fizika, Vol. 46, No. 2, pp. 122–129, March–April, 2005. Original article submitted March 9, 2004; revision submitted July 21, 2004.

 0021-8944/05/4602-0250 © 2005 Springer Science + Business Media, Inc.

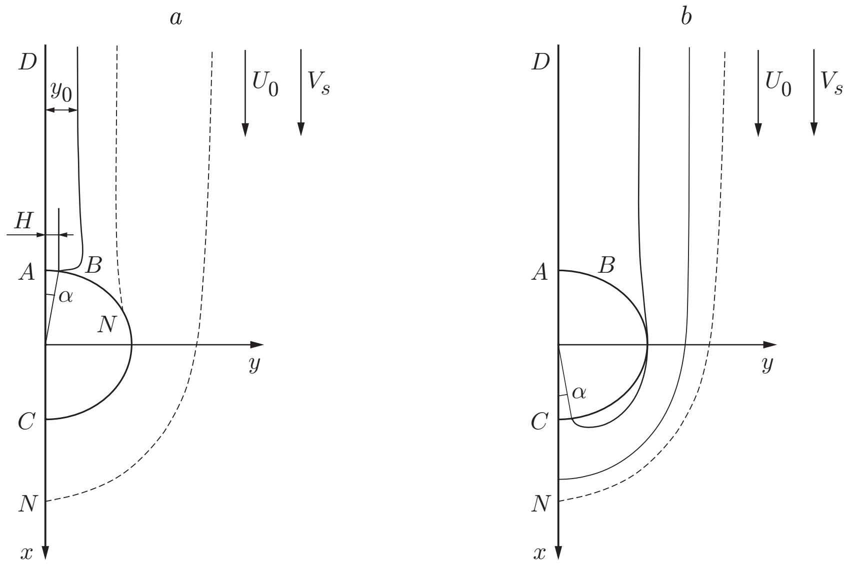

Fig. 1. Scheme of the flow with aspiration into a cylindrical sampler from a downward flow.

flow of an incompressible fluid. Based on numerical integration of the equations of particle motion in the resultant velocity field and determination of the limiting trajectories, the aspiration factor was parametrically studied for varied Stokes number, different ratios of free-stream and aspiration velocities, and different sedimentation velocities.

Formulation of the Problem. The sampler under consideration is a cylinder whose long side is perpendicular to the flow. Aerosol particles far from the sampler fall down with a uniform downward gas flow with a velocity U_0 and under the action of the force of gravity with a steady sedimentation velocity V_s. In the Cartesian coordinate system (X, Y) with the X axis directed vertically downward, the cylinder cross section is a circle with the polar coordinates r_0, θ. A slot of width $2H$ is located on the upper or lower part of the cylinder, along its generatrix; aspiration of aerosol from the incoming flow is performed through this slot.

In many cases important for practice, the problem of a two-dimensional flow of the carrier medium can be considered with acceptable accuracy within the framework of the model of a steady potential flow of an incompressible fluid. We introduce a complex variable $Z = X + iY$, a complex potential of the flow $W = W(z)$, and dimensionless quantities $z = Z/r_0$, $x = X/r_0$, $y = Y/r_0$, $h = H/r_0$, and $R = U_0/U_a$. The slot size is normally much smaller that the cylinder radius; hence, $h \ll 1$, and the flow through the cross section of the slot can be presented as the flow through an arc $\{|z| = 1,\ \pi - \alpha \leqslant \theta \leqslant \pi + \alpha\ (\alpha \ll 1)\}$ with a flow rate $q = 2HU_a$, where U_a is the aspiration velocity (mean velocity of the gas flow at the entrance of the sampler orifice). We assume that the flow potential on this arc is constant. The remaining part of the circumference is impermeable.

Figure 1 shows the scheme of the right half of the flow $y \geqslant 0$; Figs. 1a and 1b correspond to sampler positions with the orifice oriented upward and downward, respectively. The dashed curves show the streamlines separating the aspired gas and the gas flowing around the cylinder. These streamlines pass through the point N with zero velocity of the flow. The limiting trajectories (solid curves) separate the aspired particles and the particles that do not enter the sampler.

Velocity Field of the Carrier Medium and Equations of Motion of the Particles. We consider the case where the sampler orifice is oriented upward. The function

$$\varsigma = (z + 1/z)/2 \tag{1}$$

yields the mapping of the flow region in the plane $z = x + iy$ onto the upper half-plane ς. Under the condition that $-\cos\alpha < n \leqslant 1$, the stagnation point N ($\varsigma = n$) lies on the circumference. If $n > 1$, then the point N is located on the x axis. The flow region in the plane $w = W/(U_a r_0) = \varphi + i\psi$ corresponds to the quadrangle DABND with angles π, $\pi/2$, $\pi/2$, and 2π.

According to the Christoffel–Schwarz integral [13], we have

$$w(\varsigma) = 2c \int (\varsigma + 1)^{-1/2}(\varsigma + \cos\alpha)^{-1/2}(\varsigma - n)\, d\varsigma. \tag{2}$$

Based on (1), (2), the complex potential $w(z)$ and the complex-conjugate velocity of the flow $\chi(z) = dw/dz = u_x - iu_y$ with allowance for the condition $\chi(\infty) = R$ are written as

$$w(z) = R\Big[\frac{1+z}{z}\,(z^2 + 2z\cos\alpha + 1)^{1/2} - 2(1 + \cos\alpha + 2n)\ln\frac{1 + z + (z^2 + 2z\cos\alpha + 1)^{1/2}}{z^{1/2}}\Big]; \tag{3}$$

$$\frac{dw}{dz} = \frac{R(z-1)(z^2 - 2nz + 1)}{z^2(z^2 + 2z\cos\alpha + 1)^{1/2}}. \tag{4}$$

Taking into account that the difference in stream-function values at the points A and B equals the flow rate through the arc AB and that $\cos\alpha = \sqrt{1-h^2}$, we obtain the following relation from Eq. (3):

$$n = (Q - \sqrt{1-h^2} - 1)/2, \qquad Q = h/(\pi R). \tag{5}$$

Relations (4), (5) allow us to represent the Cartesian coordinates of the carrier-phase flow velocity u_x, u_y in terms of the coordinates of the point z and the parameters h and R. According to these relations, the zero velocity is reached at the x axis at the points $x = 1$ and $x = n + (n^2 - 1)^{1/2}$ for $n > 1$ or on the circumference at the points $x = n$ and $y = (1 - n^2)^{1/2}$ for $n < 1$.

Let $\alpha \to 0$, $h \to 0$, $R \to 0$, and the flow rate Q through the sampler remain unchanged. Then, $n = Q/2 - 1$, and formulas (3) and (4) are presented in the form

$$\frac{w(z)}{R} = \frac{W(z)}{U_0 r_0} = z + \frac{1}{z} - Q\ln\frac{(z+1)^2}{z};$$

$$\frac{1}{R}\frac{dw}{dz} = \frac{1}{U_0 r_0}\frac{dW}{dz} = 1 - \frac{1}{z^2} - Q\Big(\frac{2}{z+1} - \frac{1}{z}\Big). \tag{6}$$

Expression (6) yields the velocity field for the point-sink model examined in [3, 8].

The dimensionless complex-conjugate velocity of the flow in the case of aspiration from calm air can be obtained from formulas (4) and (5) as $R \to 0$:

$$\frac{dw}{dz} = \frac{h}{\pi}\,\frac{1-z}{z(z^2 + 2z\sqrt{1-h^2} + 1)^{1/2}}.$$

The complex potential and the complex-conjugate velocity of the carrier-phase flow field for the downward-oriented sampler orifice (see Fig. 1b) are written in the form

$$w(z) = R\Big[\frac{z-1}{z}\,(z^2 - 2z\cos\alpha + 1)^{1/2} - 2(2m - 1 - \cos\alpha)\ln\frac{z - 1 + (z^2 - 2z\cos\alpha + 1)^{1/2}}{z^{1/2}}\Big],$$

$$\frac{dw}{dz} = \frac{R(z+1)(z^2 - 2mz + 1)}{z^2(z^2 - 2z\cos\alpha + 1)^{1/2}}, \qquad m = \frac{1}{2}\,(Q + 1 + \sqrt{1-h^2}).$$

Under the assumption of the Stokes law of drag and neglect of all forces except for the drag force and the force of gravity, the dimensionless equations of motion of non-interacting aerosol particles are written as

$$\frac{dv_x}{dt} = \frac{u_x - v_x}{\mathrm{St}} + \frac{v_s}{\mathrm{St}}, \qquad \frac{dv_y}{dt} = \frac{u_y - v_y}{\mathrm{St}},$$
$$\frac{dx}{dt} = v_x, \qquad \frac{dy}{dt} = v_y, \tag{7}$$

where v_x and v_y are the dimensionless Cartesian components of the particle velocity, t is the time, $\mathrm{St} = \tau U_a/r_0$ is the Stokes number, $\tau = \rho_p\delta^2/(18\mu)$ is the particle-relaxation time, ρ_p is the density of the particle material, δ is the particle diameter, μ is the dynamic viscosity of the carrier medium, $v_s = V_s/U_a$ is the dimensionless velocity of sedimentation due to gravity, and $V_s = \tau g$ (g is the acceleration of gravity). In addition to the Stokes number introduced above, the problems of aerosol aspiration from a moving gas involve the modified Stokes number $\mathrm{St}_0 = \tau U_0/r_0 = \mathrm{St}\, R$.

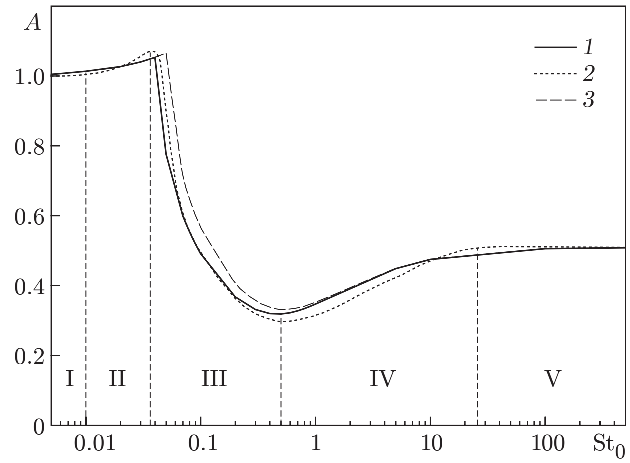

Fig. 2. Aspiration factor A as a function of St_0 for $R = 0.51$ and $h = 0.016$: the curves show the results obtained by the model with allowance for the finite size of the input orifice (1), by the point-sink model (2), and by the model with allowance for viscosity with $\mathrm{Re} = 10^4$ [6] (3).

Solving Eqs. (7) with the initial conditions at $t = 0$

$$v_x = R + v_s, \quad v_y = 0, \qquad x = x_0, \quad y = y_0 \tag{8}$$

allows us to calculate the trajectory of the aerosol particle.

The aspiration factor A is determined as the ratio of the concentration C_a of particles in the aerosol flow at the entrance of the aspirating orifice to the concentration of particles far from the sampler C_0. The condition of the balance of aspired particles whose trajectories are bounded by the limiting trajectory with the initial coordinate Y_0 far from the sampler and at the orifice entrance is

$$C_0(U_0 + V_s)2Y_0 = C_a q. \tag{9}$$

With allowance for Eq. (9), we obtain

$$A = C_a/C_0 = (U_0 + V_s)Y_0/(U_a H) = R_1 y_0/h, \tag{10}$$

where $R_1 = R + y_s$, $y_0 = Y_0/r_0$.

Calculation Results. Using the above-described model and the point-sink model, we studied aerosol aspiration from a downward flow with allowance for the force of gravity. The limiting trajectory was found by two methods: method of iterations and method of the boundary-value problem proposed in [14]. The method of iterations implies solving the Cauchy problem (7), (8) many times and determining the particle trajectory incident onto the edge of the input orifice. The particle is assumed to be captured if its trajectory intersects the arc AB. In the method of the boundary-value problem, in Eqs. (7), the condition for the particle velocity far from the sampler is set at one end of the time interval of particle motion, and the particle coordinates are equal to the coordinates of the input-orifice edge on the other end of this time interval. The results calculated by the two methods turned out to be coincident; the method of the boundary-value problem, however, was more efficient.

The difference between the model proposed and the point-sink model starts to manifest in an immediate vicinity of the input orifice. The point-sink model on the cylinder yields an infinitely high velocity in the sink and, hence, an overrated velocity in the immediate vicinity of the sink, which can affect the accuracy of calculating the aspiration factor. The proposed analytical model, which takes into account the finite size of the aspirating orifice, predicts a more realistic distribution of the velocity field in the immediate vicinity of the sampler.

Some results of the calculations performed are described below. The aspiration factor as a function of the Stokes number St_0 for sampling from a moving flow is plotted in Fig. 2. The dependence of the aspiration factor on the Stokes number with five distinct domains [6], typical of samplers with a blunt head, is observed. The aspiration efficiency is close to unity in the domain of low Stokes numbers (domain I) when the particle inertia is not yet manifested. With increasing Stokes number, the aspiration factor slightly increases (domain II). After

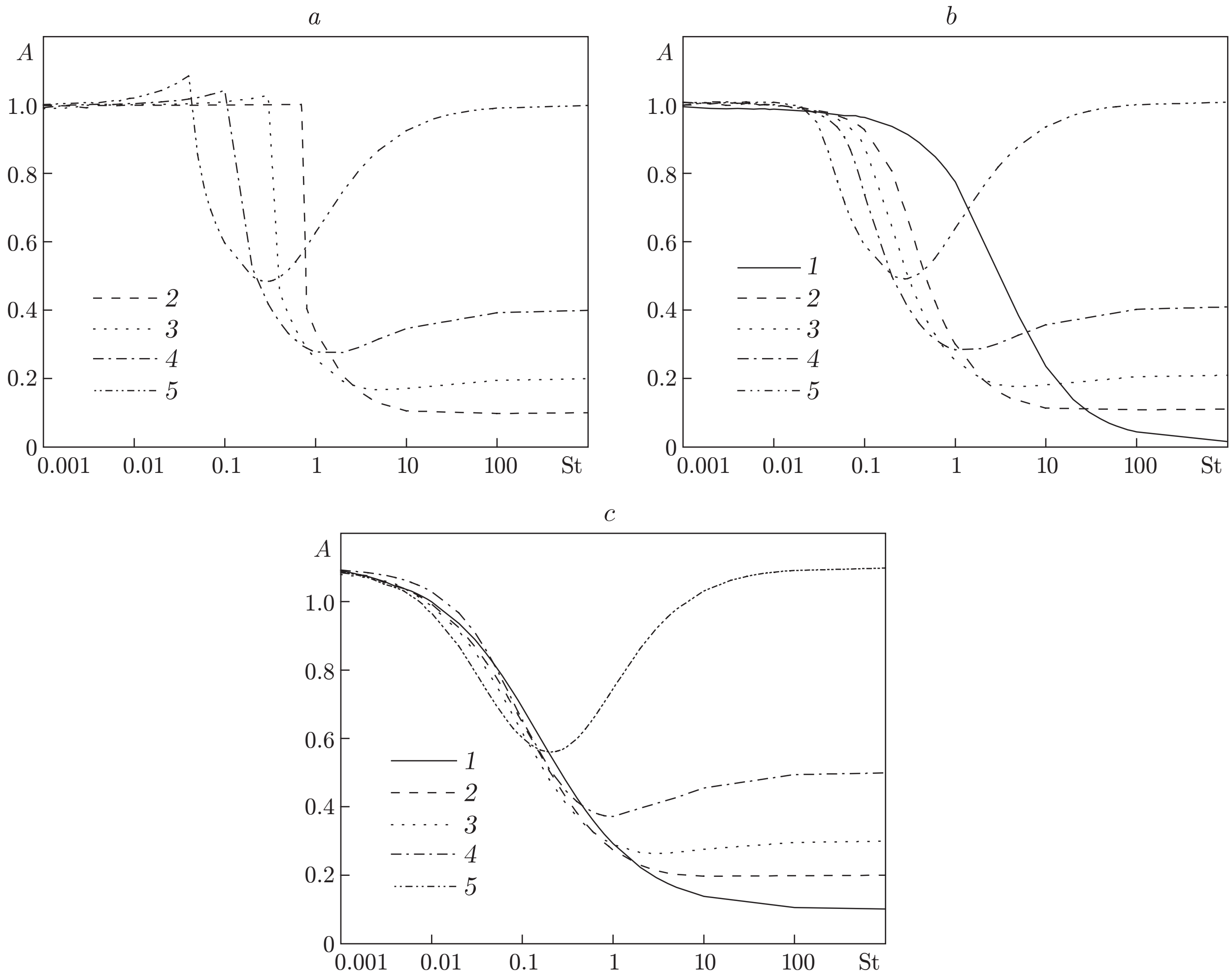

Fig. 3. Curves $A(\mathrm{St})$ for $v_s = 0$ (a), 0.01 (b), and 0.1 (c), and $R = 0$ (1), 0.1 (2), 0.2 (3), 0.4 (4), and 1 (5).

the maximum, the aspiration efficiency decreases to a minimum value (domain III). Particles with Stokes numbers corresponding to domain IV have such a large value of inertia that they hardly experience the influence of the gas velocity ahead of the sampler. The aspiration efficiency increases to an asymptotic value corresponding to the case of strongly inertial particles (domain V). As $\mathrm{St} \to \infty$, the initial ordinate of the limiting trajectory coincides with the orifice half-width $y_0 = h$; hence, according to Eq. (10), the aspiration factor becomes equal to the ratio of free-stream and aspiration velocities.

Figure 2 shows that the model proposed and the point-sink model predict similar results in the domains of rather high and low Stokes numbers (domains IV, V, I, and II). A noticeable difference in results is observed in the range of intermediate Stokes numbers (domain III). The model with allowance for the finite size of the input orifice yields better agreement with results obtained in the approximation of the viscous fluid.

The velocity of indoor air flows is normally lower than 0.1–0.2 m/sec, i.e., we can assume that the range of variation of wind velocity is $U_0 = 0$–0.2 m/sec. Experimental data for the case of sampling of aerosol particles into a thin-walled tube from a low-velocity downward flow with aspiration velocities $U_a = 0.2$–13 m/sec are given in [15]. Thus, we can assume that the range of interest for studying indoor aspiration is the range of the ratios of wind and aspiration velocities $R = 0$–1. Note, for these velocities and typical sizes of cylindrical samplers, the influence of inertia on the aspiration factor is noticeable beginning from a particles size of 10 μm.

The aspiration factor is plotted in Fig. 3 as a function of the Stokes number for $v_s = 0$, 0.01, and 0.1 with a varied ratio of free-stream and aspiration velocities. In the absence of the gravity force (Fig. 3a), the aspiration

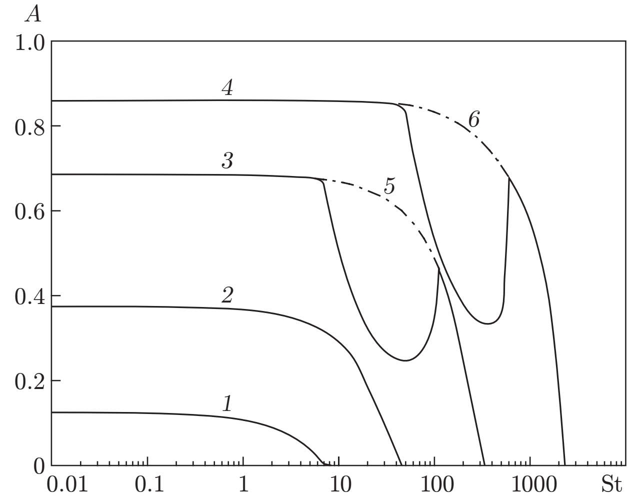

Fig. 4. Curves $A(\mathrm{St})$ for a sampler with a downward-oriented orifice for $R = 0$ and $v_s = 0.014$ (1), 0.01 (2), 0.005 (3 and 5), and 0.002 (4 and 6) and $h = 0.016$ (1–4) and 0.16 (5 and 6).

factor changes from unity to R as the Stokes number changes from zero to infinity. With decreasing R, the decrease in the aspiration factor becomes more intense, and the maximum and minimum for intermediate values of St disappear in the distribution $A(\mathrm{St})$. This is related to the change in the flow-field character ahead of the sampler for small R. The contribution of the flow from the sink to the total field of velocities exceeds the influence of the flow around the cylinder. For $v_s \neq 0$, all curves emanate from the limiting value $A = 1 + v_s$ as $\mathrm{St} \to 0$. With increasing Stokes number, the aspiration factor decreases to a certain value; the smaller R, the lower this value. In this range, the aspiration efficiency is determined by the inertial behavior of particles in the sink field and by sedimentation. With increasing St, the inertia of particles acquired in the incoming flow begins to manifest, and the curves tend to $A = R + v_s$ as $\mathrm{St} \to \infty$, either monotonically or passing through a minimum. In the case $v_s = 0.01$, the aspiration factor depends on R for intermediate values of the Stokes number as well (Fig. 3b). The zone of the decrease in the aspiration factor with decreasing ratio of wind and aspiration velocities is shifted toward higher Stokes numbers. For higher sedimentation velocities, the curves $A(\mathrm{St})$ corresponding to different values of R are close to the corresponding dependence in the case of aspiration from calm air and are little different from each other on the decreasing segment (Fig. 3c).

For a downward-oriented orifice of the sampler and in the presence of a downward gas flow, the potential-flow model used, apparently, predicts only qualitatively correct results because of the significant influence of viscosity and the probability of gas-flow separation behind the cylinder. The calculated aspiration factor in calm air for this case is described below. Figure 4 shows the dependence $A(\mathrm{St})$ for $R = 0$ and different values of the normalized sedimentation velocity v_s and h. In such orientation of the sampler, the cylinder head starts to screen the flux of incident particles. For a certain combination of the Stokes number and sedimentation velocity, the screening effect yields a zero aspiration factor, and aerosol particles are not aspired.

For inertia-free particles with allowance for screening, the aspiration factor can be presented in the form [4]

$$A = 1 - v_s(1/h - 1). \tag{11}$$

The calculated values of the aspiration factor for $\mathrm{St} \to 0$ correspond to formula (11). Under the condition $A = 0$, it follows from Eq. (11) that $v_s = h/(1 - h)$ is the value of sedimentation velocity on exceeding which the particles do not enter the sampler. The solid curves in Fig. 4 correspond to the orifice width $h = 0.016$. For $v_s = 0.005$ and $v_s = 0.002$, the behavior of $A(\mathrm{St})$ is nonmonotonic, with a crevasse in the region of intermediate values of St. The peak observed in the behavior of the aspiration factor is explained by sedimentation of particles attracted by the flow from the sink onto the cylinder near the sampler orifice. Thus, this effect is manifested for low sedimentation velocities in the case of a small width of the input orifice. An increase in the orifice width ($h = 0.16$) with an unchanged mass flow of the sink leads to aspiration of those particles that would hit the cylinder in the case of a small width of the orifice (dot-and-dashed curves 5 and 6 in Fig. 4). Outside the domain of Stokes numbers where sedimentation on the lower part of the cylinder is possible (curves 3 and 5; 4 and 6), the aspiration factors for different widths of the orifice and an identical flow rate of the sampler coincide.

Conclusions. A simple analytical model for the field of velocities of the carrier medium in the problem of aspiration into a two-dimensional cylindrical sampler is proposed. The model takes into account the finite size of the input orifice and yields good agreement with the model with allowance for viscous effects. In the problem of aspiration from a downward low-velocity flow and from calm air, the force of gravity becomes an important factor that affects the aspiration factor. In the limiting cases of inertia-free and strongly inertial particles, the additive contribution of the force of gravity is proportional to the steady sedimentation velocity. For intermediate values of the Stokes number, the aspiration factor is determined by the simultaneous action of inertia and gravity forces. For the sampler with a downward-oriented orifice, small values of the orifice width and sedimentation velocity can lead to sedimentation of particles on the lower part of the cylinder, responsible for crevasses in the distribution of the aspiration factor as a function of the Stokes number.

This work was supported by the Russian Foundation for Basic Research (Grant No. 02-01-00836) and by the Ministry of Education of the Russian Federation (Grant No. A03-2.10-613, 2003).

REFERENCES

1. J. H. Vincent, *Aerosol Sampling: Science and Practice*, Wiley and Sons, London (1989).
2. V. M. Voloshchuk, *Introduction into Hydrodynamics of Coarsely Disperse Aerosols* [in Russian], Gidrometeoizdat, Leningrad (1971).
3. S. J. Dunnett and D. B. Ingham, *The Mathematics of Blunt Body Sampling. Lecture Notes in Engineering*, Springer-Verlag, Berlin (1988).
4. C. N. Davies, "Movement of dust particles near a horizontal cylinder containing a sampling orifice," *Brit. J. Appl. Phys.*, **18**, 653–656 (1967).
5. S. J. Dunnett and D. B. Ingham, "A mathematical theory to two-dimensional blunt body sampling," *J. Aerosol Sci.*, **17**, No. 5, 839–853 (1986).
6. I. P. Chung and D. Dunn-Rankin, "Numerical simulations of two-dimensional blunt body sampling in viscous flow," *J. Aerosol Sci.*, **23**, 217–232 (1992).
7. I. P. Chung and D. Dunn-Rankin, "The effects of bluntness and orientation on two dimensional samplers in calm air," *Aerosol Sci. Technol.*, **19**, 371–380 (1993).
8. S. J. Dunnett, "Particle motion in the vicinity of a bulky sampling head operating in calm air," *Aerosol Sci. Technol.*, **36**, 308–317 (2002).
9. I. P. Chung and D. Dunn-Rankin, "Experimental investigation of air flow around blunt aerosol samplers," *J. Aerosol Sci.*, **28**, No. 2, 289–305 (1997).
10. I. P. Chung, T. Trinh, and D. Dunn-Rankin, "Experimental investigation of a two-dimensional cylindrical sampler," *J. Aerosol Sci.*, **25**, No. 5, 935–955 (1994).
11. S. J. Dunnett and J. H. Vincent, "A mathematical study of aerosol sampling by an idealised blunt sampler oriented at an angle to the wind: The role of gravity," *J. Aerosol Sci.*, **31**, 1187–1203 (2000).
12. R. S. Galeev and S. K. Zaripov, "Theoretical study of aerosol sampling by an idealised sampler in calm air," *J. Aerosol Sci.*, **34**, No. 9, 1135–1150 (2003).
13. M. A. Lavrent'ev and V. V. Shabat, *Methods of the Theory of Functions of Complex Variables* [in Russian], Nauka, Moscow (1973).
14. R. S. Galeev and S. K. Zaripov, "Deposition of aerosol particles on a sphere: the role of gravity," *Aerosol Sci. Technol.*, **37**, 325–329 (2003).
15. S. A. Grinshpun, G. N. Lipatov, and A. G. Sutugin, "Sampling errors in cylindrical nozzles," *Aerosol Sci. Technol.*, No. 12, 716–740 (1990).